Melittin Interaction with Sulfated Cell Surface Sugars†

Gabriela Klocek and Joachim Seelig*

Department of Biophysical Chemistry, Biozentrum, University of Basel, Klingelbergstrasse 50/70, CH-4056 Basel, Switzerland

Received November 13, 2007; Revised Manuscript Received December 18, 2007

ABSTRACT: Melittin is a 26-residue cationic peptide with cytolytic and antimicrobial properties. Studies on the action mechanism of melittin have focused almost exclusively on the membrane-perturbing properties of this peptide, investigating in detail the melittin−lipid interaction. Here, we report physical−chemical studies on an alternative mechanism by which melittin could interact with the cell membrane. As the outer surface of many cells is decorated with anionic (sulfated) glycosaminoglycans (GAGs), a strong Coulombic interaction between the two oppositely charged molecules can be envisaged. Indeed, the present study using isothermal titration calorimetry reveals a high affinity of melittin for several GAGs, that is, heparan sulfate (HS), dermatan sulfate, and heparin. The microscopic binding constant of melittin for HS is 2.4×10^5 M^{-1}, the reaction enthalpy is $\Delta H^0_{melittin} = -1.50$ kcal/mol, and the peptide-to-HS stoichiometry is ∼11 at 10 mM Tris, 100 mM NaCl at pH 7.4 and 28 °C. $\Delta H^0_{melittin}$ is characterized by a molar heat capacity of $\Delta C_P^0 = -227$ cal mol^{-1} K^{-1}. The large negative heat capacity change indicates that hydrophobic interactions must also be involved in the binding of melittin to HS. Circular dichroism spectroscopy demonstrates that the binding of the peptide to HS induces a conformational change to a predominantly α-helical structure. A model for the melittin−HS complex is presented. Melittin binding was compared with that of magainin 2 and nisin Z to HS. Magainin 2 is known for its antimicrobial properties, but it does not cause lysis of the eukaryotic cells. Nisin Z shows activity against various Gram-positive bacteria. Isothermal titration calorimetry demonstrates that magainin 2 and nisin Z do not bind to HS (5–50 °C, 10 mM Tris, and 100 mM NaCl at pH 7.4).

Melittin is the major protein component of the bee venom of the honey bee *Apis melifera* and has hemolytic activity and antmicrobial properties (*1, 2*). Melittin is composed of 26 amino acid residues with the sequence H_2N-GIGAV-LKVLTTGLPALISWIKRKRQQ-$CONH_2$. It is a cationic peptide in which the amino terminal end is composed predominantly of hydrophobic amino acids (residues 1–20), whereas the carboxyl terminal end has a stretch of mostly hydrophilic amino acids (residues 21–26). This uneven distribution of hydrophobic and polar residues gives melittin its amphipathic properties. Melittin is water soluble and exhibits strong affinity to lipid membranes. It is largely unstructured in water, but forms an α-helix upon binding to lipid membranes (*3*). Melittin is very sensitive to the solution conditions and can adopt different conformations and aggregation states in aqueous solution. At low peptide concentration and low ionic strength, melittin occurs as a monomer with a mostly random coil conformation. When the peptide concentration and/or the salt concentration are increased, melittin aggregates into a tetramer with a high content of α-helix structure (*4–6*).

The interaction of melittin with the lipid membrane has been investigated extensively, both experimentally and theoretically (*7–13*). Various studies show that the interaction depends on lipid composition, peptide concentration, hydration level, and membrane potential (*14*). The affinity of melittin is larger for membranes composed of negatively charged lipids than for zwitterionic lipids, indicating that hydrophobic as well as electrostatic interactions are involved in the binding of melittin to membranes (*8, 15*).

Two different action mechanisms have been proposed for the hemolytic activity of melittin. In one model, melittin acts on the lipid membrane through pore formation. Some studies envisage a barrel-stave mechanism (*16–18*), and others suggest the formation of toroidal pores (*13, 19*). The alternative detergent-like model assumes that melittin behaves much like a detergent. At low concentrations of peptide, the molecules are oriented parallel to the surface of the bilayer. Increase of the peptide concentration causes aggregation and reduction of the bilayer thickness. When a critical concentration is reached, the peptide changes its orientation and disrupts the bilayer, inducing disintegration of the membrane into micelles (*20–23*). A decision between the various models is not possible at present, and the influence of various parameters, such as the peptide-to-lipid ratio, membrane composition, temperature, hydration or buffer compositions, needs to be considered (*23*).

As melittin carries a net positive charge of $z = 5$, it can be expected that it not only interacts with lipid membranes but also binds to polyanions such as sulfate-carrying glycosaminoglycans (GAGs),[1] which are found on almost all

† Supported by the Swiss National Science Foundation Grant 3100-107793.

* To whom correspondence should be addressed. Tel: +41-61-267 2190. Fax: +41-61-267 2189. E-mail: joachim.seelig@unibas.ch.

[1] Abbreviations: DS, dermatan sulfate; HS, heparan sulfate; GAG, glycosaminoglycan; ITC, isothermal titration calorimetry; CD, circular dichroism spectroscopy; CHO, Chinese hamster ovary.

10.1021/bi702258z CCC: $40.75
Published on Web 01/26/2008

cell surfaces. This interaction has not been investigated before, but related studies with two melittin analogues have recently been reported (*24*).

In the present study, we have used high-sensitivity isothermal titration calorimetry (ITC) to obtain a complete thermodynamic characterization of melittin binding to three different glycosaminoglycans, namely, heparan sulfate, heparin, and dermatan sulfate. In addition, the structural changes of melittin induced by binding to these polyanions were followed by circular dichroism (CD) spectroscopy. Finally, we have compared the specificity of melittin binding to GAGs with analogous measurements with magainin 2 and nisin Z, two amphiphatic and antimicrobial peptides with lipid binding properties similar to those of melittin.

MATERIALS AND METHODS

Materials. Melittin from bee venom was purchased from SIGMA (St. Louis, MO). Synthetic melittin and magainin 2 were purchased from BACHEM AG (Bubendorf BL, Switzerland) (purity >97% by reverse phase HPLC). The peptides were used without further purification. The concentration of melittin in aqueous solution was determined by UV spectroscopy at 280 nm using an absorption coefficient of 5570 M^{-1} cm^{-1} (*5*). Nisin Z was kindly provided by Dr. E. Breukink from Utrecht University. Heparan sulfate (HS), sodium salt (from porcine intestinal mucosa; average molecular weight, 13,655 Da; sulfur content 5.51%), and dermatan sulfate (DS), sodium salt (from porcine intestinal mucosa; average molecular weight, 41,400 Da; sulfur content 6.85%) were from Celsus Laboratories (Cincinnati, OH). Low molecular weight heparin, sodium salt (from porcine intestinal mucosa; average molecular weight, 3000) was from SIGMA (St. Louis, MO). All other chemicals were of analytical or reagent grade. Tris buffer (10 mM tris(hydroxymethyl)aminoethane at pH 7.4) was prepared from 18 MΩ water obtained from a NANOpure A filtration system. NaCl concentrations were variable (50 to 250 mM) and are specified in the legends of each figure. The samples were degassed immediately before use.

Isothermal Titration Calorimetry. All measurements were made with a Microcal VP-ITC calorimeter (Microcal, Northampton, MA). Titrations were performed by injecting 10 μL aliquots of the glycosaminoglycan solution into the calorimeter cell (V_{cell} = 1.4037 mL) containing peptide at a concentration of typically 90–100 μM. The concentrations of the injected glycosaminoglycan solution were about 100 μM for HS, 35 μM for DS, and 500 μM for heparin.

The heats of dilution were determined in control titrations by injecting glycosaminoglycan solution into pure buffer. The heats of dilution were small (approximately −1 to 1 μcal) and were included in the final analysis. Raw data were processed using the Origin software provided with the instrument. The temperature was set as indicated in the legends of the figures. All measurements were performed in Tris buffer (10 mM, pH 7.4) with varying NaCl concentrations.

Circular Dichroism Spectroscopy. CD measurements of melittin in the absence and presence of glycosaminoglycan (buffer 10 mM Tris and 100 mM NaF at pH 7.4) were made using a Chirascan CD spectrometer (Applied Photophysics Ltd., Leatherhead, UK). A quartz cuvette with a path length of 0.1 cm was used. All spectra were corrected by subtracting the buffer baseline. Results are reported as mean residue ellipticity in units of deg cm^2 $dmol^{-1}$. The percentage of peptide secondary structure was estimated from a computer simulation based on the reference spectra obtained by Reed and Reed (*25*).

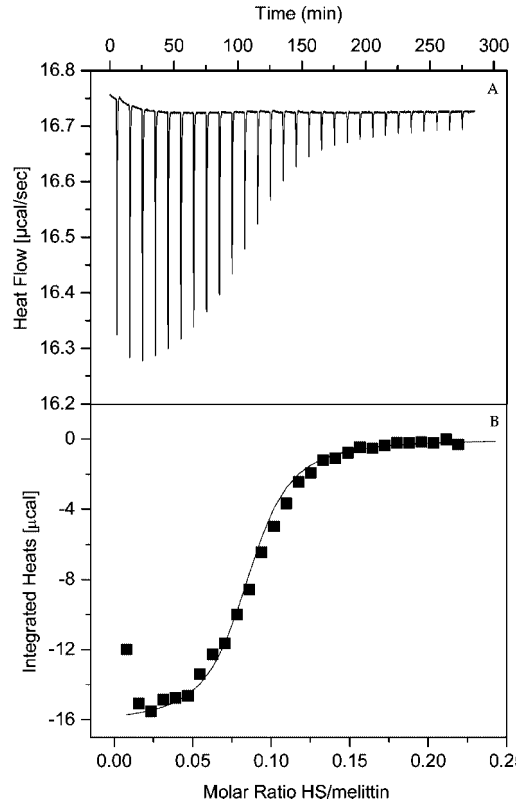

FIGURE 1: Titration of HS into synthetic melittin. (A) Calorimetric trace obtained at 28 °C by titration of HS (100 μM) into a solution of melittin (91 μM). Each peak corresponds to the injection of 10 μL of HS into the calorimeter cell. (B) Heats of reaction (integrated from the calorimetric trace) plotted as a function of the HS/melittin ratio. The solid line is the best fit to the experimental data (■) using the binding model described by eqs 1–3 with the following parameters: $\Delta H^0_{melittin} = -1.50$ kcal/mol, $K = 2.4 \times 10^5$ M^{-1}, and $n = 11$. Buffer: 10 mM Tris and 100 mM NaCl at pH 7.4.

RESULTS

Binding of Melittin to HS. Figure 1A shows a representative calorimetric heat flow trace obtained by the titration of synthetic melittin with HS (at 28 °C). A 91 μM solution of melittin was filled into the calorimeter cell (V_{cell} = 1.4037 mL), and 10 μL aliquots of a 100 μM HS solution were injected at 10 min intervals. The corresponding titration curve is shown in Figure 1B, where the reaction heats are plotted as a function of the HS/melittin molar ratio. The reaction heats were obtained by integration of the titrations peaks shown in Figure 1A and were corrected for the heats of dilution obtained in a separate HS-into-buffer titration.

Figure 1 demonstrates an *exothermic* reaction at 28 °C. The heats measured after the first few injections are rather constant with $h_i \cong -15.5$ μcal per injection. As melittin is much in excess over HS, it is reasonable to assume that all injected HS (10 nmol per injection) is completely bound to melittin. The molar heat of reaction of HS can thus be evaluated as $\Delta H^0_{HS} = -15.5$ μcal/10 nmol = −15.5 kcal/mol HS. As more HS is injected, the concentration of free melittin decreases, and the heats of reaction become progres-

Table 1: Titration of Synthetic Melittin with HS[a]

T (°C)	n	K (M^{-1})	$\Delta H^0_{melittin}$ (kcal/mol)	$\Delta G^0_{melittin}$ (kcal/mol)	$T\Delta S^0_{melittin}$ (kcal/mol)	ΔS^0_{mol} (cal/mol K)
5	11.2	1.9×10^5	4.60	−6.71	11.31	40.7
10	13.5	2.0×10^5	2.80	−6.86	9.66	34.1
15	12.5	2.2×10^5	2.30	−7.04	9.34	32.4
28	11.0	2.4×10^5	−1.50	−7.41	5.91	19.6
37	10.4	2.3×10^5	−2.20	−7.60	5.40	17.4
50	9.5	2.0×10^5	−6.10	−7.83	1.73	5.4

[a] Thermodynamic parameters as a function of temperature in buffer are shown (10 mM Tris 100 mM NaCl at pH 7.4).

sively smaller. When all peptide is bound to HS, the residual heats of the last few injections are due to the dilution of HS into buffer. The molar binding enthalpy of melittin is then determined from the total heat released in the titration (~170.8 μcal) and the amount of peptide in the calorimeter cell (127.7 nmol). For the experiment shown in Figure 1, the heat of reaction is $\Delta H^0_{melittin} \approx -1.34$ kcal/mol. The ratio $\Delta H^0_{HS}/\Delta H^0_{melittin} = 11.5$ provides the number of melittin molecules bound per HS. This result can also be derived from the midpoint of the transition (Figure 1B) at HS/mel = 0.086, the reciprocal value of which is $n = 11.6$.

For a complete thermodynamic characterization of the binding process including the free energy, ΔG^0, and the entropy, ΔS^0, the calorimetric data were analyzed with a multisite binding model, which was also used to describe the binding equilibrium of other peptides to HS (*26, 27*). In this model, a long polymer such as HS is visualized as a macromolecule with n independent and equivalent binding sites for a ligand such as melittin. The binding model is represented by the following equation:

$$\frac{[P]_b}{[HS]_t} = \frac{nK[P]}{1 + K[P]} \quad (1)$$

[P] and $[P]_b$ are the concentrations of free and bound melittin, respectively, $[HS]_t$ is the total concentration of heparan sulfate, K is the intrinsic binding constant, and n is the number of melittin molecules bound per heparan sulfate polysaccharide chain.

Because of mass conservation, the concentration of bound peptide can be described by the following equation:

$$[P]_b = \frac{1}{2}\left(\frac{1}{K} + [P]_t + n[HS]_t\right) - \frac{1}{2}\sqrt{\left(\frac{1}{K} + [P]_t + n[HS]_t\right)^2 - 4n[HS]_t[P]_t} \quad (2)$$

The index t denotes the total concentration of peptide and heparan sulfate in the calorimeter cell after each injection step. The peptide concentration changes during the titration with HS because of dilution effects.

The concentration of bound peptide is linked to the calorimetric data by the following equation:

$$\delta Q_i = \Delta H^0_{melittin} \delta [P]_{b,i} V \quad (3)$$

where δQ_i is the heat absorbed or released at the ith injection. $\Delta H^0_{melittin}$is the peptide binding enthalpy, $\delta[P]_{b,i}$ is the change (increase) in *bound* peptide concentration upon injection i, and V is the volume of the calorimeter cell. The solid line in Figure 1B is the best least-squares fit to the data using 1−3 with the following set of parameters: $n = 11$, $K = 2.4 \times 10^5$ M^{-1}, and $\Delta H^0_{melittin} = -1.50$ kcal/mol (cf. Table 1). n and $\Delta H^0_{melittin}$ are consistent with the simple calculations given above. In addition, the multisite binding model provides the binding constant K and, in turn, the free energy of binding $\Delta G^0_{melittin}$.

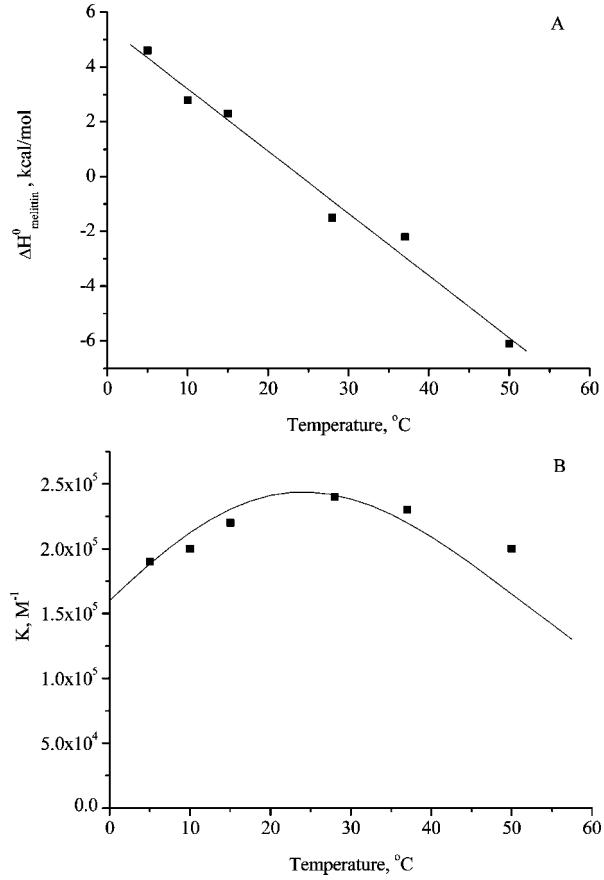

FIGURE 2: Temperature dependence of the thermodynamic parameters. (A) $\Delta H^0_{melittin}$ for synthetic melittin binding to HS. Linear regression analysis of the experimental data in yields $\Delta H^0_{melittin} = 5.47 - 0.227T$ (°C) (solid line). (B) Binding constant K_0. The solid line in B is the predicted temperature dependence of K_0 based on the van't Hoff equation and using the above regression formula for $\Delta H^0_{melittin}$ (T). Buffer: 10 mM Tris and 100 mM NaCl at pH 7.4.

Calorimetric titrations were performed at various temperatures in the range of 5–50 °C. Table 1 summarizes the thermodynamic parameters derived by using the binding model described above.

The binding stoichiometry melittin/HS varies between 9.5 to 13.5 and becomes smaller at higher temperatures. The reaction enthalpy shows an even stronger temperature dependence and changes from *endothermic* below 15 °C ($\Delta H^0_{melittin} > 0$) to *exothermic* above this temperature. $\Delta H^0_{melittin}$ decreases linearly with increasing temperature as demonstrated in Figure 2A. The slope of the straight line yields a molar heat capacity change of $\Delta C^0_{P,melittin} = -227$ cal mol^{-1} K^{-1}. This result is quite different from previous HS binding studies obtained with cell-penetrating peptides such as TAT and R_9, which reveal positive heat capacity values of $\Delta C^0_{P,TAT}$ = 135 cal mol^{-1} K^{-1} (*27*) and $\Delta C^0_{P,R9} = 155$ cal mol^{-1} K^{-1} (*26*), respectively. The negative ΔC^0_P is indicative of a hydrophobic contribution to the binding process, whereas the positive ΔC^0_P values are the signature for the electrostatic interactions (*28*). The solid line in Figure 2B describes the predicted temperature dependence of the binding constant

Table 2: Thermodynamic Parameters for Synthetic Melittin Binding to Heparin and DS[a]

T (°C)	n	K (M^{-1})	$\Delta H^0_{melittin}$ (kcal/mol)	$\Delta G^0_{melittin}$ (kcal/mol)	$T\Delta S^0_{melittin}$ (kcal/mol)
heparin					
5	2.6	0.9×10^6	5.40	−7.57	12.97
10	2.6	1.0×10^6	3.50	−7.77	11.27
37	2.7	0.9×10^6	−3.90	−8.45	4.55
dermatan sulfate					
10	30.5	1.1×10^6	3.90	−7.82	11.72
28	40.0	1.2×10^6	−0.90	−8.37	7.47
37	38.0	1.0×10^6	−2.50	−8.51	6.01

[a] Buffer: 10 mM Tris and 100 mM NaCl at pH 7.4.

K based on van't Hoff's law $d\ln K/dT = \Delta H^0_{melittin}/RT^2$, taking into account the temperature dependence of the reaction enthalpy as $\Delta H(T) = \Delta H^0 + \Delta C^0_P (T - T_0)$.

Table 1 demonstrates that the reaction is completely entropy driven below 15 °C as $\Delta H^0 > 0$ but becomes mainly enthalpy driven at 50 °C. However, the free energy of binding is fairly constant, which is also reflected in the weak temperature dependence of the binding constant K (Figure 2B). A plot of ΔH^0 versus $T\Delta S^0$ yields a straight line in the temperature interval measured (not shown). The large heat capacity change then provides an explanation for this enthalpy–entropy compensation phenomenon, that is, the linear correlation between ΔH^0 and $T\Delta S^0$. The temperature coefficient of ΔH^0 is ΔC^0_P, and that of $T\Delta S^0$ is close to $\Delta C^0_P + \Delta S^0_P$. As $\Delta C^0_P \approx \Delta S^0$ (cf. Table 1), the two thermodynamic parameters ΔH^0 and $T\Delta S^0$ vary in parallel.

The binding constant at 28 °C is $K = 2.4 \times 10^5$ M^{-1} and is of the same order of magnitude as that observed for other peptide−HS equilibria measured previously (TAT, R_9, mel-SH, ri-mel-SH). This is rather unexpected since the electrostatic and hydrophobic contributions appear to vary quite considerably between the different peptides.

We have studied the specificity of melittin binding with two further GAGs, that is, heparin and dermatan sulfate (DS). Heparin is composed of the same monosaccharide building blocks as HS but has a higher degree of sulfation. In DS, glucosamine is replaced by the galactosamine residue. ITC titration curves exhibit the same pattern as those observed for HS at identical temperatures, and the binding isotherms can again be described by the multisite binding model of eqs 1–3. The results are shown in Table 2.

For both GAGs, the binding constants K and the reaction enthalpies $\Delta H^0_{melittin}$ are larger than those obtained for HS. For heparin and DS, the binding constants are of the order of 10^6 M^{-1}. The peptide molar binding enthalpies, $\Delta H^0_{melittin}$ at 37 °C are −3.90 kcal/mol for heparin and −2.50 kcal/mol for DS. Likewise, the molar heat capacity changes are more negative with $\Delta C^0_P = -285.1$ cal mol^{-1} K^{-1} for heparin and −241.3 cal mol^{-1} K^{-1} for DS. The main difference found between these glycosaminoglycans is, however, the binding stoichiometry. The number of binding sites for melittin at 37 °C is 2.7 for heparin, 10.4 for HS, and 38 for DS. However, this result is not surprising as the three polyanions have quite different chain lengths. A better comparison is the number of binding sites per 1 kDa. With this normalization, one finds ∼0.76 binding sites for HS, ∼0.90 for heparin, and ∼0.92 for DS per 1 kDa molecular weight.

ITC Studies with Magainin 2 and Nisin Z. Melittin belongs to a large group of amphipathic peptides that either disrupt the lipid bilayer in a detergent-like manner or form pores or related structures. The question then arises if the interaction with sulfated glycosaminoglycans is a general property of these microbial antibiotics. As an additional example we have, therefore, studied the binding of magainin 2 and nisin Z to HS. Magainin 2 is secreted from the skin of the african clawed frog, *Xenopus leavis*. It consists of 23 amino acid residues and has a net positive charge of $z = 4$. Magainin 2 is known for its antimicrobial properties, but in contrast to melittin does not cause lysis of the eukaryotic cells (*29*). Nisin Z, secreted by the lactic bacteria *Lactoccocus lactis*, is a 34 amino acid residue peptide also with a net positive charge $z = 4$, with several unusual dehydro residues and five thioether-bridged lanthionines (*30*). It finds application as a food preservative and exerts its activity against Gram-positive bacteria. The interactions of magainin 2 and nisin Z with HS were studied here with isothermal titration calorimetry. We performed titrations of HS into magainin 2 (110–120 μM) and nisin Z (50 μM) solutions at three different temperatures in 10 mM Tris and 100 mM NaCl at pH 7.4. The data did not reveal any binding of magainin 2 or nisin Z to heparan sulfate in the temperature of 5–50 °C. At least in this series of experiments, binding to GAGs appears to be a unique property of melittin.

Table 3: Effect of NaCl on the Thermodynamic Parameters of HS Binding to Bee Venom Melittin at 28 °C[a]

NaCl (mM)	n	K (M^{-1})	$\Delta H^0_{melittin}$ (kcal/mol)	$\Delta G^0_{melittin}$ (kcal/mol)	$T\Delta S^0_{melittin}$ (kcal/mol)
50	9.8	1.0×10^6	−1.40	−8.26	6.86
	9.5	1.0×10^6	−1.50	−8.26	6.76
100[b]	8.5	3.0×10^5	−1.70	−7.54	5.84
	10.0	3.5×10^5	−1.20	−7.64	6.44
150	10.0	1.0×10^5	−1.50	−6.89	5.39
	10.0	1.0×10^5	−1.50	−6.89	5.39
250	10.0	2.5×10^4	−1.40	−6.06	4.66
	10.0	3.0×10^4	−1.30	−6.17	4.87

[a] Buffer: 10 mM Tris and variable concentrations of NaCl at pH 7.4. [b] The small differences to the data in Table 1 can be explained by the different sources of melittin: melittin from natural source in Table 3 and synthetic melittin in Table 1.

Effect of NaCl on the Interaction between HS and Melittin. As ionic interactions play an important role in the binding of melittin to HS, we performed HS-into-melittin titrations at various NaCl concentrations. The thermodynamic parameters obtained at 28 °C and evaluated with the binding model described above are summarized in Table 3.

As expected for electrostatic interactions, the binding affinity of HS to melittin decreases with increasing salt content of the buffer. We have analyzed the salt dependence of the binding constant with a popular model for protein−polyelectrolyte interactions (*31*). HS is a highly charged poly anion, but a considerable fraction of its sulfate groups is probably neutralized by Na^+ because of counterion condensation (*32*). Upon binding of melittin, the counterions are released into the bulk solution as described by the following reaction scheme:

$$HS(Na)_z + n\text{Mel} \rightarrow HS \cdot \text{Mel}_n + z\text{Na}^+ \quad (4)$$

with the corresponding equilibrium

$$K_T = \frac{[HS \cdot \text{Mel}_n][\text{Na}^+]^z}{[HS(\text{Na})_z][\text{Mel}]^n} = K[\text{Na}^+]^z \quad (5)$$

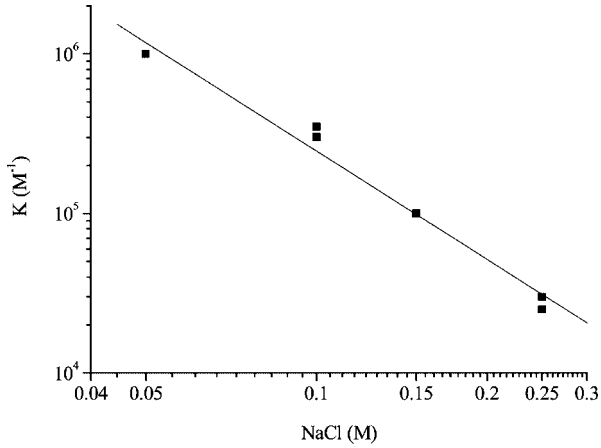

FIGURE 3: Salt dependence of the interaction between HS and bee venom melittin. The binding constant (K_0) for HS binding to melittin was determined as a function of NaCl concentration in Tris buffer (10 mM Tris at pH 7.4) from ITC measurements at 28 °C. The K values are plotted as a function of the NaCl concentration on a log/log scale. Linear regression analysis of the experimental data yields log $K = 3.14 - 2.26$ log [NaCl] (solid line).

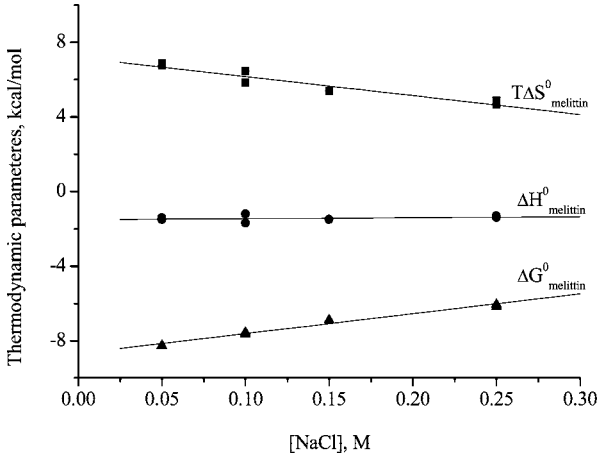

FIGURE 4: Dependence of $\Delta G^0_{melittin}$, $\Delta H^0_{melittin}$, and $T\Delta S^0_{melittin}$ on NaCl concentration in Tris buffer (10 mM Tris at pH 7.4) at 28 °C for the interaction of bee venom melittin with HS.

K_T is the binding constant at 1 M Na^+ concentration and is usually described as $K_{nonionic}$, as ionic interactions are much reduced at this concentration. However, K is the actual binding constant derived directly from the ITC experiment, which varies with the Na^+ concentration (Table 3). Taking the logarithm on both sides of equation (*5*) and rearranging gives the following expression:

$$\log K = \log K_T - z\log[Na^+] \quad (6)$$

A plot of the experimental log K as a function of log [Na^+] should be linear with slope z and y-intercept log K_T. Figure 3 shows this linear relationship for the melittin/HS system. Linear regression analysis yields $z_{Na^+} = -2.26$ (about two Na^+ ions are released when melittin binds to HS), and the nonionic binding constant $K_T = 1.4 \times 10^3$ M^{-1}.

The variation of the thermodynamic parameters with salt concentration is displayed in Figure 4. The reaction enthalpy $\Delta H^0_{melittin}$ is independent of NaCl concentration, but $\Delta S^0_{melittin}$ decreases with increasing ionic strength. This indicates that the salt dependence of $\Delta G^0_{melittin}$ is entropic in origin. This was also observed for the binding of oligolysines to duplex DNA (*33*) and single-stranded polynucleotides (*34, 35*), and for the binding of tripeptide-containing lysine to heparin (*36*).

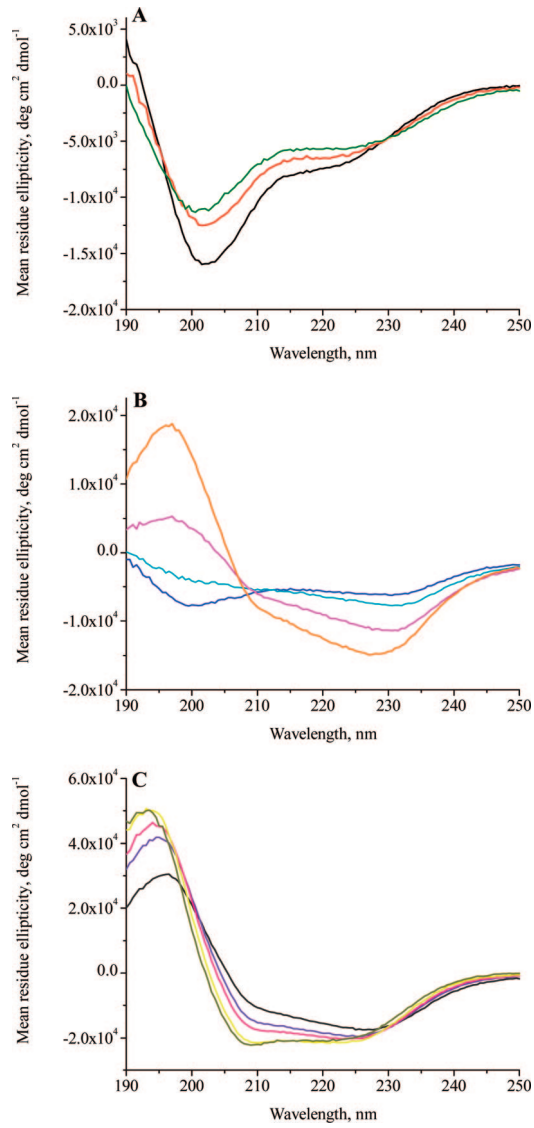

FIGURE 5: CD spectra monitoring conformational changes in bee venom melittin upon the addition of heparan sulfate. Mean residue ellipticity values of melittin (44.3 μM) in the absence and upon titration with heparan sulfate (22 μM) are plotted as a function of wavelength. (A) Black, melittin; red, HS/melittin 0.01; green, HS/melittin 0.02. (B) Blue, HS/melittin 0.04; cyan, HS/melittin 0.06; magenta, HS/melittin 0.08; orange, HS/melittin 0.10. (C) Dark gray, HS/melittin 0.12; violet, HS/melittin 0.16; pink, HS/melittin 0.20; yellow, HS/melittin 0.30; dark yellow, HS/melittin 0.50. Buffer: 10 mM Tris and 100 mM NaF at pH 7.4.

Structural Properties of Melittin Binding to HS. Structural changes of synthetic melittin induced by binding to HS were followed by circular dichroism (CD) spectroscopy. The CD spectra of melittin in buffer (10 mM Tris and 100 mM NaF at pH 7.4 at room temperature) were measured at a peptide concentration of 44 μM and were titrated with a 22 μM solution of HS.

The corresponding CD spectra are displayed in Figure 5. For better visualization, they are separated into three regions of low (A), middle (B), and high (C) HS content. Figure 5 demonstrates that melittin adopts an essentially random coil (rc) conformation in the absence of HS. The random coil content is 60%, but α-helix and β-structure contribute 22% and 19%, respectively. Upon addition of HS, the α-helix

FIGURE 6: Schematic representation of melittin−HS interactions. HS with 29 disaccharide units (♦♢), with total length of ∼290 Å. Melittin helix length is ∼37 Å, and the diameter is ∼11 Å.

content increases steeply to about 56% at a HS-to-melittin ratio of ∼0.12, whereas further addition of HS induces a slow increase to 63% α-helix at a HS-to-melittin ratio of 0.5. The conformational change involves several structural transitions and cannot be described by a two-state equilibrium over the full range. However, at low HS-to-melittin ratios (0–0.02), a two-state equilibrium is observed with isosbestic points at $\lambda \simeq 195$ and 228 nm (Figure 5A). For high HS-to-melittin ratios ($0.06 \leq r \leq 0.1$), a second two-state transition region appears with an isosbestic point at $\lambda \simeq 208$ nm (Figure 5C). The conformational changes in the intermediate region $0.04 > r > 0.1$ are characterized by a steep increase and decrease of β-turn structure (cf. Figure 5B). Analogous CD titrations of melittin were performed with dermatan sulfate and heparin. The corresponding CD spectra are qualitatively and quantitatively very similar to those obtained for HS.

Helix formation in aqueous solution is an exothermic process with a reaction enthalpy of $\Delta H^0_{\text{helix}} \simeq -0.9$ to -1.1 kcal/mol (*37, 38*). The increase in the α-helix content of melittin by 41%, corresponding to 10.7 amino acid residues, should thus entail a reaction enthalpy of about −10 kcal/mol. In addition, the electrostatic interaction of the 3 Lys and 2 Arg side chains with the HS sulfate groups could also make an exothermic contribution. However, the experimental result $\Delta H^0_{\text{mel}} \simeq -1.5$ kcal/mol is far different from this theoretical expectation. As an explanation, it may be speculated that the helix−coil transition in the melittin−HS system has an enthalpy close to zero or that the enthalpy is even slightly positive. The classical example for a positive ΔH_{helix} is the coil-to-helix transition of poly(γ-benzy-L-glutamate) (PBGL) with $\Delta H^0_{\text{helix}} = +890$ cal/mol per residue (*39*), taking place in ethylene dichloride/dichloroacetic acid (DCA). The random coil conformation is stabilized by specific PBGL−DCA interactions that are broken up at higher temperatures. Analogously, it can be argued that the binding of melittin to HS requires the removal of water molecules from melittin and/or HS, which is an endothermic process. The release of water would make a positive contribution to entropy. We have measured the CD spectra of melittin bound to HS as a function of temperature in the range 5–40 °C. We observe a 15% reduction in the mean residual ellipticity, while the shape of the spectra remains unchanged. As the CD spectrum of a perfect helix is itself sensitive to temperature (*37*), the observed change is consistent with the literature data and excludes a melting of the helix. This measurement also supports the conclusion that the enthalpy of the coil-to-helix transition of the melittin−HS system is close to zero. It may further be noted that $\Delta H^0_{\text{helix}}$ was found to decrease in mixed H_2O/trifluoroethanol (TFE) solvents (*37*) assuming a value $\Delta H^0_{\text{helix}} = -0.1$ kcal/mol residue in pure TFE.

DISCUSSION

We observe a strong binding of melittin to three different GAGs, but no binding of nisin Z or magainin 2. Nisin Z has lysine residues at positions 12, 22, and 34. The cationic charges are spaced far apart, and they cannot act in concert. For magainin 2 with lysines at positions 4, 10, 11, and 14, the electric charge density is higher, but the spatial distances appear not to agree with the stereochemistry of the sulfated sugars. Melittin, however, has a cluster of 4 cationic charges at amino acids 21–24 followed by 2 glutamines at 25–26, which could make additional H-bridges. The significance of the spatial arrangement of the lysine and arginine residues is supported by a related study of synthetic peptides interacting with the heparin binding domain of the heparin/heparan sulfate-interacting protein. The all-L-amino acid peptide and the all-D-amino acid version of the same peptide had the same efficacy as that of the agents for neutralization of the anticoagulant activity of heparin. In contrast, a peptide with a scrambled peptide sequence had no effect. The spatial pattern of the charged amino acids was found to be of critical significance (*40*).

Structural Model. The HS employed in the present binding studies is composed of about 29 disaccharide units, on the basis of an average molecular weight of 13,655 Da for HS and 464 Da for a sulfated disaccharide unit. However, a sulfur content of 5.51% leads to 23.5 SO_4^- groups. As each disaccharide unit also carries a -COO^- group, the total anionic charge of HS is about $z_{\text{HS}} = -53 \pm 5$. Charge neutralization is achieved if 10–11 melittin molecules are bound, provided each melittin contributes 5 positive charges. This is only possible if melittin with its helical axis is extended parallel to the HS chain, as 4 cationic amino acids are clustered at the C-terminus, whereas the fifth (Lys-7) is located at the other end of the molecule. Figure 6 shows a schematic representation of approximate scale of a complex consisting of HS (29 disaccharide units) and 11 melittin molecules in helical conformation. In a three-dimensional picture, the melittin molecules should be wrapped around the disaccharide string producing hydrophobic interactions between neighboring melittins. The HS itself may also adopt a curled conformation. Inspection of the crystal structure of melittin (*41*) reveals a distance of 9.22 Å (10.05 Å) between the $^+NH_3$ groups of Lys 21−Arg 24 (Arg 22−Lys 23). The distance between 2 sulfate groups on heparin has been estimated as 8–8.6 Å (see Figure 1D in ref *42*). As there is no perfect match of distances, both melittin and HS must rearrange their structure to produce optimum ion pair formation.

The binding stoichiometry of melittin ($n = 11$) is distinctly smaller than those of the analogues [Cys^1] melittin ($n = 15.5 \pm 0.7$) and retro-inverso [Cys^1] melittin (14 ± 1.5) investigated previously (*24*). The replacement of the N-terminal glycine of melittin by cystein in the analogues appears to modify the binding properties such that only the cationic

-KRKR- carboxy terminus but not K-7 in the hydrophobic N-terminal region binds to HS. A larger number of ligands compared to natural melittin is hence required to guarantee the electroneutrality of the HS−melittin−analogue complexes. The increased ligand density requires a different packing model for the two melittin analogues. While the charged N-terminus is associated with the HS chain, part of the C-terminus must extend away from the chain axis into the aqueous phase.

Thermodynamic and Structural Aspects of Melittin Binding to HS. Melittin has a high affinity to HS as shown by the calorimetric data presented here. The binding constant at 28 °C is $K = 2.4 \times 10^5$ M^{-1}, corresponding to a dissociation constant of 4.2 μM.

At low temperatures (≤15 °C), the melittin−HS interaction is endothermic, and binding is exclusively driven by entropic forces. Above 15 °C, the reaction enthalpy changes to exothermic, but even at 50 °C, the entropy term accounts for 35% of the total free energy ΔG^0. The large negative heat capacity change of $\Delta C^0_{P,\text{melittin}} = -227$ cal/mol suggests hydrophobic interactions as the source of the entropy gain. The binding affinity of natural melittin is somewhat smaller than those of its analogues [Cys^1]melittin (6.5×10^5 M^{-1}) and retro-inverso [Cys^1]melittin (4.0×10^5 M^{-1}) (*24*).

Coulombic interactions between the cationic peptide and the anionic HS make an essential contribution to the free energy of binding. The Mel-HS binding constant decreases with increasing salt concentration to $K = 1.3 \times 10^3$ M^{-1} (extrapolated) at 1 M NaCl. Compared to $K = 3 \times 10^5$ M^{-1} at 100 mM NaCl, this corresponds to a reduction of 43% in the free energy ΔG. The change in ΔG^0 is essentially entropic in nature as the reaction enthalpy ΔH^0 is virtually independent of salt concentration.

Melittin binding to HS may be compared with the interaction of a basic cyclic peptide to heparin for which an extensive ITC study was performed (*43*). The brain natriuretic peptide (BNP) has a cyclic structure, which is related to an acidic fibroblast growth factor. BNP contains 32 amino acids with 3 Lys and 4 Arg and is comparable in size and charge to melittin. The binding constant to heparin is $K = 2 \times 10^5$ M^{-1} (100 mM NaCl and 50 mM ΔPO_4^-, 25 °C, pH 7.4), which is very similar to melittin binding to HS (3×10^5 M^{-1}). However, heparin carries more sulfate groups than HS, and the BNP−heparin interaction normalized to the charge density is thus weaker than the melittin−HS interaction. The reaction enthalpy is in the range of -3.2 kcal/mol $\leq \Delta H_{BNP} \leq -0.4$ kcal/mol depending on salt concentration. The molar heat capacity is $\Delta C_p = 1$ kcal mol^{-1} K^{-1} (referred to heparin) and thus opposite in sign to that of the melittin−HS reaction ($\Delta C_{p,\text{melittin}} = -227$ cal mol^{-1} K^{-1}). The positive heat capacity suggest strong polar interactions. This is, however, contradicted by the rather small salt dependence of the BNP−heparin binding constant. The ionic contribution was estimated as only 6%, which is much lower than that found for melittin−HS or other heparin-binding proteins (*44–48*). Only 0.5 Na^+ ions are replaced upon BNP binding.

BNP binding to heparin is accompanied by a distinct protonation reaction. Five H^+ are bound upon complex formation (*43*). We have, therefore, investigated the buffer dependence of the melittin−HS reaction. The reaction enthalpy varies only slightly between –1.5 kcal/mol (TRIS) over −1.8 kcal/mol (phosphate) to −2.6 kcal/mol (MOPS, HEPES), but is not correlated with the buffer dissociation enthalpies. A proton uptake or release can thus be excluded. The binding constant in phosphate buffer is only 1.1×10^5 M^{-1} (50 mM ΔPO_4^- and 100 mM NaCl), which can be explained by a specific interaction between melittin and ΔPO_4^- (*49*).

In elucidating the cytolytic action mechanism of melittin, most researchers have focused on the interaction of melittin with the lipid part of the cell membrane, and only a few reports have discussed the role of glycosaminoglycans. It was suggested, for example, that melittin forms a complex with heparin secreted from mast cells, neutralizing, in turn, the cytotoxic effect of melittin (*50*). Complexes between melittin and heparin result in an enhanced immune response to the peptide present in the complex (*51*). Melittin-induced cell lysis has been described in some detail for red blood cells (*2*), human lymphoblastoid cells (*52, 53*), or Caco-2 cells (*54*). However, the molecular mechanism of cell lysis was not addressed in these studies.

The present data suggest that the melittin−GAG interaction should be investigated as a potential target initiating cell lysis, enhancing, perhaps, the melittin−lipid interaction. As a first step in this direction, we have investigated the effect of melittin on two related Chinese hamster ovary (CHO) cell lines, one of which has a reduced content of sulfated GAGs. We have used the pgsA-745 mutant cell line (ATCC, Manassas, VA), which is deficient in xylosyltransferase, the enzyme responsible for the initiation of chondroitin sulfate and heparan sulfate biosynthesis *in vivo* (*55*). As a control, we used CHO K1 cells (ATCC, Manassas, VA). After incubation with melittin, the cell viability was determined with CytoTox-One Homogeneous Membrane Integrity Assay (Promega Corporation, Madison, WI) according to the manufacturer's instructions. Differences in the cytotoxic effect of melittin for these two cell lines were observed in the range of peptide concentrations 3 to 5 μM. At 3 μM melittin, the percent cytotoxicity is 44.8 ± 4.3% for CHO K1 cells but only 31.6 ± 2% for pgsA-745 cells with reduced GAG content. Even though the main mechanism is probably the permeabilization of the lipid membrane, these data suggest that the role of GAGs cannot be ignored. A more detailed report including results from different cell lines and confocal microscopy is in preparation.

ACKNOWLEDGMENT

We thank Dr. K. Ballmer-Hofer (Paul-Scherrer-Institut, Villigen, Switzerland) for kindly providing the CHO cell lines. We are indebted to Dr. E. Breukink (University of Utrecht) for a gift of purified nisin Z.

REFERENCES

1. Habermann, E. (1972) Bee and wasp venoms. *Science 177*, 314–322.
2. Tosteson, M. T., Holmes, S. J., Razin, M., and Tosteson, D. C. (1985) Melittin lysis of red cells. *J. Membr. Biol. 87*, 35–44.
3. Vogel, H. (1981) Incorporation of melittin into phosphatidylcholine bilayers. Study of binding and conformational changes. *FEBS Lett. 134*, 37–42.
4. Bello, J., Bello, H. R., and Granados, E. (1982) Conformation and aggregation of melittin: dependence on pH and concentration. *Biochemistry 21*, 461–465.

5. Quay, S. C., and Condie, C. C. (1983) Conformational studies of aqueous melittin: thermodynamic parameters of the monomer-tetramer self-association reaction. *Biochemistry 22*, 695–700.
6. Wilcox, W., and Eisenberg, D. (1992) Thermodynamics of melittin tetramerization determined by circular dichroism and implications for protein folding. *Protein Sci. 1*, 641–653.
7. Berneche, S., Nina, M., and Roux, B. (1998) Molecular dynamics simulation of melittin in a dimyristoylphosphatidylcholine bilayer membrane. *Biophys. J. 75*, 1603–1618.
8. Beschiaschvili, G., and Seelig, J. (1990) Melittin binding to mixed phosphatidylglycerol/phosphatidylcholine membranes. *Biochemistry 29*, 52–58.
9. Dempsey, C., Bitbol, M., and Watts, A. (1989) Interaction of melittin with mixed phospholipid membranes composed of dimyristoylphosphatidylcholine and dimyristoylphosphatidylserine studied by deuterium NMR. *Biochemistry 28*, 6590–6596.
10. Glattli, A., Chandrasekhar, I., and Gunsteren, W. F. (2006) A molecular dynamics study of the bee venom melittin in aqueous solution, in methanol, and inserted in a phospholipid bilayer. *Eur Biophys J 35*, 255–267.
11. Kuchinka, E., and Seelig, J. (1989) Interaction of melittin with phosphatidylcholine membranes. Binding isotherm and lipid headgroup conformation. *Biochemistry 28*, 4216–4221.
12. Papo, N., and Shai, Y. (2003) Exploring peptide membrane interaction using surface plasmon resonance: differentiation between pore formation versus membrane disruption by lytic peptides. *Biochemistry 42*, 458–466.
13. Yang, L., Harroun, T. A., Weiss, T. M., Ding, L., and Huang, H. W. (2001) Barrel-stave model or toroidal model? A case study on melittin pores. *Biophys. J. 81*, 1475–1485.
14. Dempsey, C. E. (1990) The actions of melittin on membranes. *Biochim. Biophys. Acta 1031*, 143–161.
15. Batenburg, A. M., van Esch, J. H., and de Kruijff, B. (1988) Melittin-induced changes of the macroscopic structure of phosphatidylethanolamines. *Biochemistry 27*, 2324–2331.
16. Katsu, T., Ninomiya, C., Kuroko, M., Kobayashi, H., Hirota, T., and Fujita, Y. (1988) Action mechanism of amphipathic peptides gramicidin S and melittin on erythrocyte membrane. *Biochim. Biophys. Acta 939*, 57–63.
17. Ladokhin, A. S., Selsted, M. E., and White, S. H. (1997) Sizing membrane pores in lipid vesicles by leakage of co-encapsulated markers: pore formation by melittin. *Biophys. J. 72*, 1762–1766.
18. Rex, S., and Schwarz, G. (1998) Quantitative studies on the melittin-induced leakage mechanism of lipid vesicles. *Biochemistry 37*, 2336–2345.
19. Allende, D., Simon, S. A., and McIntosh, T. J. (2005) Melittin-induced bilayer leakage depends on lipid material properties: evidence for toroidal pores. *Biophys. J. 88*, 1828–1837.
20. Ladokhin, A. S., and White, S. H. (2001) Protein chemistry at membrane interfaces: non-additivity of electrostatic and hydrophobic interactions. *J. Mol. Biol. 309*, 543–552.
21. Monette, M., and Lafleur, M. (1995) Modulation of melittin-induced lysis by surface charge density of membranes. *Biophys. J. 68*, 187–195.
22. Shai, Y. (2002) Mode of action of membrane active antimicrobial peptides. *Biopolymers 66*, 236–248.
23. Bechinger, B., and Lohner, K. (2006) Detergent-like actions of linear amphipathic cationic antimicrobial peptides. *Biochim. Biophys. Acta 1758*, 1529–1539.
24. Goncalves, E., Kitas, E., and Seelig, J. (2006) Structural and thermodynamic aspects of the interaction between heparan sulfate and analogues of melittin. *Biochemistry 45*, 3086–3094.
25. Reed, J., and Reed, T. A. (1997) A set of constructed type spectra for the practical estimation of peptide secondary structure from circular dichroism. *Anal. Biochem. 254*, 36–40.
26. Goncalves, E., Kitas, E., and Seelig, J. (2005) Binding of oligoarginine to membrane lipids and heparan sulfate: structural and thermodynamic characterization of a cell-penetrating peptide. *Biochemistry 44*, 2692–2702.
27. Ziegler, A., and Seelig, J. (2004) Interaction of the protein transduction domain of HIV-1 TAT with heparan sulfate: binding mechanism and thermodynamic parameters. *Biophys. J. 86*, 254–263.
28. Gomez, J., Hilser, V. J., Xie, D., and Freire, E. (1995) The heat capacity of proteins. *Proteins 22*, 404–412.
29. Zasloff, M. (1987) Magainins, a class of antimicrobial peptides from Xenopus skin: isolation, characterization of two active forms, and partial cDNA sequence of a precursor. *Proc. Natl. Acad. Sci. U.S.A. 84*, 5449–5453.
30. Breukink, E., Ganz, P., de Kruijff, B., and Seelig, J. (2000) Binding of Nisin Z to bilayer vesicles as determined with isothermal titration calorimetry. *Biochemistry 39*, 10247–10254.
31. Record, M. T., Jr., Anderson, C. F., and Lohman, T. M. (1978) Thermodynamic analysis of ion effects on the binding and conformational equilibria of proteins and nucleic acids: the roles of ion association or release, screening, and ion effects on water activity. *Q. Rev. Biophys. 11*, 103–178.
32. Manning, G. S. (1978) The molecular theory of polyelectrolyte solutions with applications to the electrostatic properties of polynucleotides. *Q. Rev. Biophys. 11*, 179–246.
33. Lohman, T. M., deHaseth, P. L., and Record, M. T., Jr. (1980) Pentalysine-deoxyribonucleic acid interactions: a model for the general effects of ion concentrations on the interactions of proteins with nucleic acids. *Biochemistry 19*, 3522–3530.
34. Mascotti, D. P., and Lohman, T. M. (1992) Thermodynamics of single-stranded RNA binding to oligolysines containing tryptophan. *Biochemistry 31*, 8932–8946.
35. Mascotti, D. P., and Lohman, T. M. (1993) Thermodynamics of single-stranded RNA and DNA interactions with oligolysines containing tryptophan. Effects of base composition. *Biochemistry 32*, 10568–10579.
36. Mascotti, D. P., and Lohman, T. M. (1995) Thermodynamics of charged oligopeptide-heparin interactions. *Biochemistry 34*, 2908–2915.
37. Luo, P., and Baldwin, R. L. (1997) Mechanism of helix induction by trifluoroethanol: a framework for extrapolating the helix-forming properties of peptides from trifluoroethanol/water mixtures back to water. *Biochemistry 36*, 8413–8421.
38. Scholtz, J. M., Marqusee, S., Baldwin, R. L., York, E. J., Stewart, J. M., Santoro, M., and Bolen, D. W. (1991) Calorimetric determination of the enthalpy change for the α helix to coil transition of an alanine peptide in water. *Proc. Natl. Acad. Sci. U.S.A. 88*, 2854–2858.
39. Zimm, B. H., Doty, P., and Iso, K. (1959) Determination of the parameters for helix formation in poly-gamma-benzyl-L-glutamate. *Proc. Natl. Acad. Sci. U.S.A. 45*, 1601–1607.
40. Wang, J., and Rabenstein, D. L. (2006) Interaction of heparin with two synthetic peptides that neutralize the anticoagulant activity of heparin. *Biochemistry 45*, 15740–15747.
41. Terwilliger, T. C., and Eisenberg, D. (1982) The structure of melittin II. Interpretation of the structure. *J. Biol. Chem. 257*, 6016–6022.
42. Silvian, L., Jin, P., Carmillo, P., Boriack-Sjodin, P. A., Pelletier, C., Rushe, M., Gong, B., Sah, D., Pepinsky, B., and Rossomando, A. (2006) Artemin crystal structure reveals insights into heparan sulfate binding. *Biochemistry 45*, 6801–6812.
43. Hileman, R. E., Jennings, R. N., and Linhardt, R. J. (1998) Thermodynamic analysis of the heparin interaction with a basic cyclic peptide using isothermal titration calorimetry. *Biochemistry 37*, 15231–15237.
44. Thompson, L. D., Pantoliano, M. W., and Springer, B. A. (1994) Energetic characterization of the basic fibroblast growth factor-heparin interaction: identification of the heparin binding domain. *Biochemistry 33*, 3831–3840.
45. Olson, S. T., Halvorson, H. R., and Bjork, I. (1991) Quantitative characterization of the thrombin-heparin interaction Discrimination between specific and nonspecific binding models. *J. Biol. Chem. 266*, 6342–6352.
46. Olson, S. T., and Bjork, I. (1991) Predominant contribution of surface approximation to the mechanism of heparin acceleration of the antithrombin-thrombin reaction Elucidation from salt concentration effects. *J. Biol. Chem. 266*, 6353–6364.
47. Faller, B., Mely, Y., Gerard, D., and Bieth, J. G. (1992) Heparin-induced conformational change and activation of mucus proteinase inhibitor. *Biochemistry 31*, 8285–8290.
48. Fath, M. A., Wu, X., Hileman, R. E., Linhardt, R. J., Kashem, M. A., Nelson, R. M., Wright, C. D., and Abraham, W. M. (1998) Interaction of secretory leukocyte protease inhibitor with heparin inhibits proteases involved in asthma. *J. Biol. Chem. 273*, 13563–13569.
49. Podo, F., Strom, R., Crifo, C., and Zulauf, M. (1982) Dependence of melittin structure on its interaction with multivalent anions and with model membrane systems. *Int. J. Pept. Protein Res. 19*, 514–527.

50. Higginbotham, R. D., and Karnella, S. (1971) The significance of the mast cell response to bee venom. *J. Immunol. 106*, 233–240.

51. Kind, L. S., and Allaway, E. (1982) Enhanced IgE and IgG anti-melittin antibody formation induced by heparin-melittin complexes in mice. *Allergy 37*, 225–229.

52. Weston, K. M., Alsalami, M., and Raison, R. L. (1994) Cell membrane changes induced by the cytolytic peptide, melittin, are detectable by 90 degrees laser scatter. *Cytometry 15*, 141–147.

53. Weston, K. M., and Raison, R. L. (1998) Interaction of melittin with a human lymphoblastoid cell line, HMy2. *J. Cell. Biochem. 68*, 164–173.

54. Maher, S., and McClean, S. (2006) Investigation of the cytotoxicity of eukaryotic and prokaryotic antimicrobial peptides in intestinal epithelial cells in vitro. *Biochem. Pharmacol. 71*, 1289–1298.

55. Seelig, J. (1997) Titration calorimetry of lipid-peptide interactions. *Biochim. Biophys. Acta 1331*, 103–116.

BI702258Z